κ+λ F(ab')$_2$ for 5 min and P-PLCγ2 was quantified by intracellular flow cytometry in gated naïve ($CD20^+CD27^{neg}$) and memory ($CD20^+CD27^+$) subsets (P-PLCγ2 assay, n=10 control C/C, n=11 control C/T; n=9 T1D C/C, n=10 T1D C/T). Bars show mean fold change in mean fluorescence intensity (MFI). (C) B cells from T1D 1858T/T subjects display signaling defects. Total B cells from T1D 1858C/C and T/T subjects shown in Figure 2D were purified from previously frozen PBMC, rested overnight, then stimulated as in (B); P-PLCγ2 was quantified by intracellular flow cytometry in gated naïve $CD20^+$ $CD27^{neg}$ B cells.

Supplemental Figure 1. *Blunted BCR signaling is an inherent defect of PTPN22 1858C/T naïve B cells that is reversed by inhibition of Lyp.* (A) Total B cells from healthy control 1858C/C and C/T subjects (n=8) were purified from previously frozen PBMC, rested overnight, then stimulated with soluble anti-κ F(ab')$_2$ for 5 min and P-PLCγ2 was quantified by intracellular flow cytometry in the naïve $CD20^+CD27^{neg}$ B cell population. Each dot represents the fold change in MFI relative to the unstimulated control for a unique individual. Statistical significance was determined using an independent Student's *t* test. (B) Total B cells from 1858C/C (n=6) and C/T (n=7) subjects were purified from previously frozen PBMC, rested overnight, then treated with vehicle or 10 μM I-C11 and stimulated as in *A*, followed by intracellular staining for P-PLCγ2. Fold change in MFI for P-PLCγ2 in the presence of vehicle or I-C11 is shown in gated naïve B cells from healthy non-carriers (closed symbols) and carriers (open symbols) of 1858T. Statistical significance was determined using a paired *t* test. (C) The LypR620W-associated BCR signaling defect is recapitulated in the immature B cell line, Ramos, expressing PEP-R619W. Generation of Wt and variant PEP-expressing Ramos cells is shown. Flow cytometric and Western blot analyses of control (non-transfected) and HA-tagged Wt PEP and PEP R619W depicting similar expression levels of Wt and variant PEP following lentiviral transduction of Ramos cells. (D) Ramos cells infected with SFFV-HA-WT PEP or PEP-R619W were loaded with the indo-1 calcium binding

dye. Flux kinetics profiles are shown comparing the mean indo-1 ratio (violet/blue) of mCherry-positive (red trace) and mCherry-negative (blue trace) as a function of time before and after stimulation with anti-IgM $F(ab')_2$ (upper and lower left panels) or ionomycin (upper and lower right panels).

Supplemental Figure 2. (A) Representative gating strategy is shown of sorted naïve ($CD19^{+}CD27^{neg}CD24^{int}CD38^{int}$) and transitional ($CD19^{+}CD27^{neg}CD24^{hi}CD38^{hi}$ ) B cells following culture in the presence and absence of anti-IgM, and intracellular staining with anti-cleaved caspase-3. (B) Serum BAFF levels are similar between healthy control and T1D subjects. Individual serum BAFF levels in 53 healthy control subjects (n=28 1858 C/C; n=25 1858 C/T, range 19-45 years) and 64 age-matched T1D donors (n=46 1858 C/C; n=14 1858 C/T; and n=4 1858 T/T), as measured by ELISA. Statistical significance was determined using a one-way analysis of variance.

Supplemental Figure 3. *Receptor editing is intact in PTPN22 1858T heterozygous immature/transitional and mature B cells.* (A and B) iRS-KDE rearrangement frequencies as quantified in peripheral $Ig\kappa^{+}$ immature ($CD19^{+}CD27^{neg}CD10^{+}CD24^{hi}CD38^{hi}$) and mature ($CD19^{+}CD27^{neg}CD24^{int}CD38^{int}$ ) B cells, respectively. Data represent the iRS-KDE levels in healthy control 1858 C/C (filled circles, n=36 for immature subset, n=39 for mature subset) and 1858 C/T (open circles, n=27 for immature subset, n=30 for mature subset) subjects. (C and D) iRS-KDE rearrangement frequencies as quantified in peripheral $Ig\lambda^{+}$ immature and mature B cells, respectively. Data represent the iRS-KDE levels in healthy control 1858C/C (filled circles, n=16 for immature subset, n=18 for mature subset) and 1858C/T (open circles, n=12 for immature subset, n=17 for mature subset) subjects. Data are depicted as iRS-KDE rearrangement frequency per genome copy. Mean values are depicted as horizontal lines.

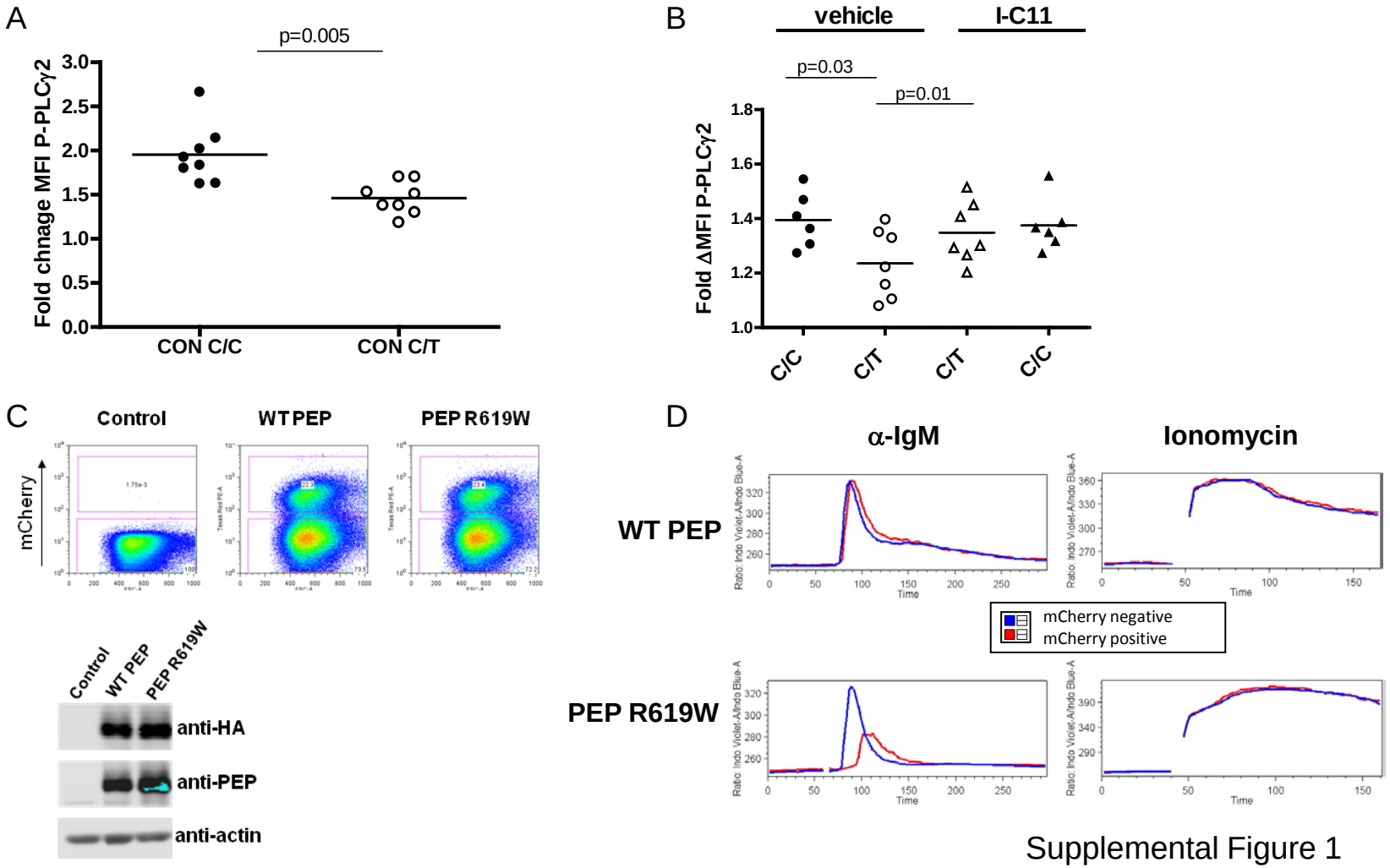


Supplemental Figure 1

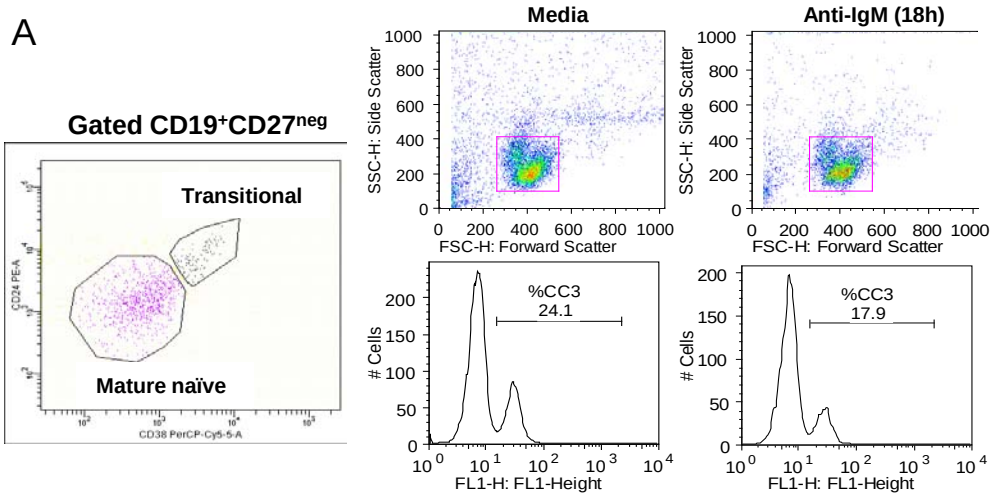


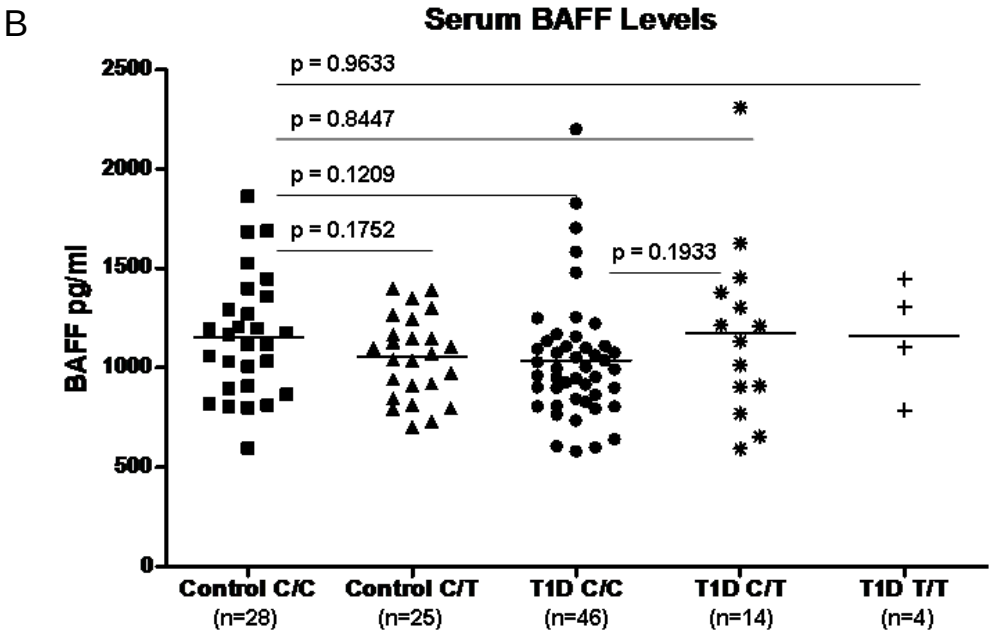


Supplemental Figure 2

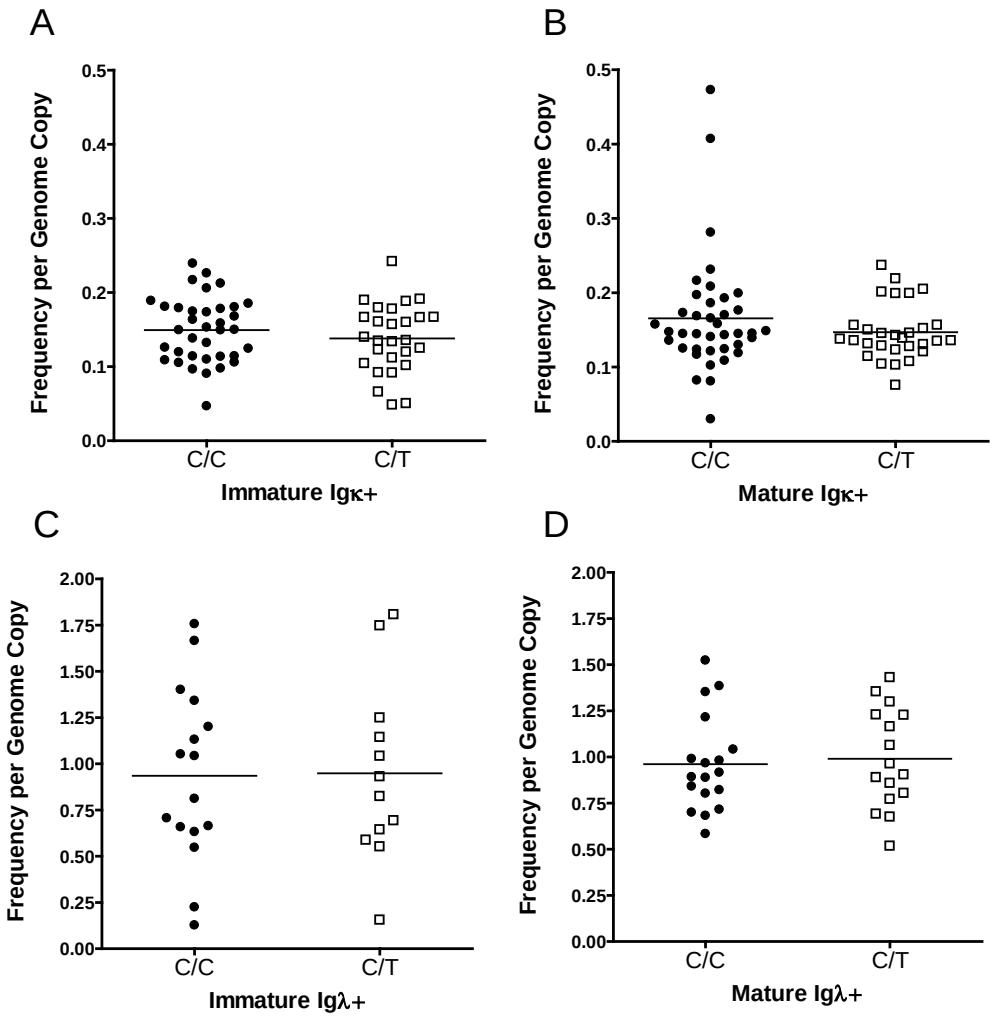


Supplemental Figure 3